REPORT DOCUMENTATION PAGE

Form Approved
OMB No. 0704-0188

1. REPORT DATE *(DD-MM-YYYY)*	2. REPORT TYPE	3. DATES COVERED *(From - To)*
01-06-2005	Journal Article	2003

4. TITLE AND SUBTITLE
Statistical Analysis of the Nonhomogeneity Detector for Non-Gaussian Interference Backgrounds

5a. CONTRACT NUMBER
N/A

5b. GRANT NUMBER
N/A

5c. PROGRAM ELEMENT NUMBER
61102F

6. AUTHOR(S)
Muralidhar Rangaswamy

5d. PROJECT NUMBER
2304

5e. TASK NUMBER
HE

5f. WORK UNIT NUMBER
2304HE01

7. PERFORMING ORGANIZATION NAME(S) AND ADDRESS(ES)
Electromagnetic Scattering Branch (AFRL/SNHE) Source Code: 437890
Electromagnetic Technology Division, Sensors Directorate
80 Scott Drive,
Hanscom AFB, MA 01731-2909

8. PERFORMING ORGANIZATION REPORT NUMBER
N/A

9. SPONSORING/MONITORING AGENCY NAME(S) AND ADDRESS(ES)
Air Force Office of Scientific Research/NM
875 North Randolph Street
Arlington, VA 22203

10. SPONSOR/MONITOR'S ACRONYM(S)
AFRL-SN-HS

11. SPONSOR/MONITOR'S REPORT NUMBER(S)
AFRL-SN-HS-JA-2003-0643

12. DISTRIBUTION/AVAILABILITY STATEMENT
APPROVED FOR PUBLIC RELEASE, DISTRIBUTION UNLIMITED.

13. SUPPLEMENTARY NOTES
ESC Public Affairs Clearance #: ESC 03-0643; Published in IEEE Transactions on Signal Proc., Vol. 53, No. 6, June 2005

14. ABSTRACT
We derive the nonhomogeneity detector (NHD) for non-Gaussian interference scenarios and present a statistical analysis of the method. The non-Gaussian interference scenario is assumed to be modeled by a spherically invariant random process (SIRP). We present a method for selecting representative (homogeneous) training data based on our statistical analysis of the NHD for finite sample support used in covariance estimation. In particular, an exact theoretical expression for the NHD test statistic probability density function (PDF) is derived. Performance analysis of the NHD is presented using both simulated data and measured data from the multichannel airborne radar measurement (MCARM) program. A performance comparison with existing NHD approaches is also included.

15. SUBJECT TERMS
EM algorithm, GIP, goodness-of-fit test, maximally invariant statistic,MLestimate,NAMF, NHD, non-Gaussian interference, SIRP, type-I error

16. SECURITY CLASSIFICATION OF:			17. LIMITATION OF ABSTRACT	18. NUMBER OF PAGES	19a. NAME OF RESPONSIBLE PERSON
a. REPORT	b. ABSTRACT	c. THIS PAGE			Muralidhar Rangaswamy
U	U	U	UU	12	19b. TELEPHONE NUMBER *(Include area code)*

Statistical Analysis of the Nonhomogeneity Detector for Non-Gaussian Interference Backgrounds

Muralidhar Rangaswamy, *Senior Member, IEEE*

***Abstract*—We derive the nonhomogeneity detector (NHD) for non-Gaussian interference scenarios and present a statistical analysis of the method. The non-Gaussian interference scenario is assumed to be modeled by a spherically invariant random process (SIRP). We present a method for selecting representative (homogeneous) training data based on our statistical analysis of the NHD for finite sample support used in covariance estimation. In particular, an exact theoretical expression for the NHD test statistic probability density function (PDF) is derived. Performance analysis of the NHD is presented using both simulated data and measured data from the multichannel airborne radar measurement (MCARM) program. A performance comparison with existing NHD approaches is also included.**

***Index Terms*—EM algorithm, GIP, goodness-of-fit test, maximally invariant statistic, ML estimate, NAMF, NHD, non-Gaussian interference, SIRP, type-I error.**

I. Introduction

An important issue in space-time adaptive processing (STAP) for radar target detection is the formation and inversion of the covariance matrix underlying the disturbance. In practice, the unknown interference covariance matrix is estimated from a set of independent identically distributed (iid) target-free training data, which is assumed to be representative of the interference statistics in a cell under test. Frequently, the training data is subject to contamination by discrete scatterers or interfering targets. In either event, the training data becomes nonhomogeneous. As a result, it is not representative of the interference in the test cell. Hence, standard estimates of the covariance matrix from nonhomogeneous training data result in severely under-nulled clutter. Consequently, constant false alarm rate (CFAR) and detection performance suffer. Significant performance improvement can be achieved by employing pre-processing to select representative training data.

The problem of target detection using improved training strategies has been considered in [1]–[5]. The impact of training data nonhomogeneity on STAP performance is considered in [5]–[8]. The works of [1]–[4], [8], [9] have addressed the use of the nonhomogeneity detector (NHD) based on the generalized inner product (GIP) measure for STAP problems involving Gaussian interference scenarios. This work was extended significantly in [10] and [11] to include the effects of finite sample support used for covariance matrix estimation. However, the corresponding problem for non-Gaussian interference scenarios has received limited attention. This is due to the fact that tractable models for correlated non-Gaussian interference have become available only in recent work [12]–[14].

In general, nonhomogeneity of training data is caused by environmental factors, such as the presence of strong discrete scatterers, dense target environments, nonstationary reflectivity properties of the scanned area, and radar system configurations such as conformal arrays, and bistatic geometries. A variety of robust adaptive signal processing methods to combat specific types of nonhomogeneities have been developed in [15]–[19].

In this paper, we concern ourselves with the problem of training data nonhomogeneity caused by dense target environments and present the NHD for non-Gaussian interference scenarios. More specifically, two p-tuple random vectors $\mathbf{x}_t$ and $\mathbf{x}_s$ having covariance matrices $\mathbf{R}_t$ and $\mathbf{R}_s$, respectively, are defined to be nonhomogeneous if $\mathbf{R}_s^{-1}\mathbf{R}_t \neq \nu\mathbf{I}$, where $\mathbf{I}$ denotes the $p \times p$ identity matrix, and ν is an arbitrary positive scale factor. In other words, the random vectors are defined to be nonhomogeneous if they do not share the same covariance structure. This issue can be readily treated by examining the eigenvalues of $\mathbf{R}_s^{-1}\mathbf{R}_t$ when $\mathbf{R}_t$ and $\mathbf{R}_s$ are known. However, $\mathbf{R}_t$ and $\mathbf{R}_s$ are seldom known in practice, rendering the eigenvalue analysis infeasible. Therefore, we concern ourselves with the problem of obtaining the NHD test for non-Gaussian interference scenarios, where the covariance matrix is estimated from finite training data support.

Specifically, we derive the NHD for non-Gaussian interference scenarios, which can be modeled by spherically invariant random processes (SIRP) and present a statistical analysis of the resultant NHD test. Section II presents the relevant mathematical preliminaries. In Section III, we discuss the issues of covariance matrix estimation using finite data as well as the use of a maximally invariant test statistic for the NHD. Furthermore, we present a statistical analysis of the NHD and show that a formal goodness-of-fit test can be constructed for selecting homogeneous training data. The basis of our NHD strategy lies in characterizing the statistics pertaining to homogeneous SIRP clutter scenarios and rejecting realizations departing from these statistics. Performance analysis is discussed in Section IV. A performance comparison with existing NHD tests is also included therein. Conclusions and future research directions are outlined in Section V.

In general, the problem of nonhomogeneity detection for SIRPs is complicated by the fact that the underlying SIRP co-

Manuscript received June 10, 2003; revised February 15, 2004. This work was supported by the Air Force Office of Scientific Research (AFOSR) under projects 2304E8 and 2304IN and by in-house research programs at Air Force Research Laboratory. Portions of this paper were presented at the 2002 IEEE Radar conference, Long Beach, CA, April 2002. The associate editor coordinating the review of this manuscript and approving it for publication was Prof. Yuri I. Abramovich.

The author is with the Air Force Research Laboratory/SNHE, Hanscom Air Force Base, MA 01731-2909 USA (e-mail: Muralidhar.Rangaswamy@hanscom.af.mil).

Digital Object Identifier 10.1109/TSP.2005.847843

variance matrix and characteristic probability density function (PDF) are unknown. Knowledge of the SIRP characteristic PDF is assumed in this paper as a first step toward addressing the problem. This information can be gained from estimates of the first order PDF obtained from experimental data using histogram or moment techniques [20]. A significant performance penalty is incurred if this information is unavailable. This fact is illustrated through an example in Section IV.

The main contributions of this paper are summarized below.

1) Reduce the NHD problem for SIRP interference scenarios to one of testing whether two data sets share a common covariance structure but have different levels by proper use of the maximum likelihood estimate of the covariance matrix.
2) Provide a formal goodness-of-fit test using a scale invariant test statistic.
3) Introduce analytical expressions for the NHD PDF, which enable calculation of the threshold setting for the NHD test.
4) Analyze the performance of the NHD test using simulated and measured radar data.
5) Compare the performance with existing NHD tests, which demonstrates superior performance of the NHD test of this paper in both SIRP as well as Gaussian scenarios.

II. Preliminaries

Let $\mathbf{x} = [x_1\ x_2\ \ldots x_M]^T$ denote a complex spherically invariant random vector (SIRV) having zero mean, positive definite Hermitian covariance matrix $\mathbf{R}$ and characteristic PDF $f_V(v)$. The PDF of $\mathbf{x}$ is given by [21]

$$f(x) = \pi^{-M}|\mathbf{R}|^{-1}h_{2M}(q) \tag{1}$$

where $|.|$ denotes determinant, and

$$q = \mathbf{x}^H\mathbf{R}^{-1}\mathbf{x}$$
$$h_{2M}(w) = \int_0^\infty v^{-2M}\exp\left(-\frac{w}{v^2}\right)f_V(v)dv. \tag{2}$$

Every SIRV admits a representation of the form [22] $\mathbf{x} = \mathbf{z}V$, where z has a complex-Gaussian PDF $CN(0,\mathbf{R})$, and V is a statistically independent random variable with PDF $f_V(v)$. Consequently, the covariance matrix of $\mathbf{x}$ is given by $\mathbf{R}_x = \mathbf{R}E(V^2)$. In practice, $\mathbf{R}$ and $f_V(v)$ are unknown. For the purpose of this paper, we assume knowledge of $f_V(v)$ and treat the problem of nonhomogeneity detection with respect to unknown $\mathbf{R}$. Validity of the SIRP model for clutter encountered in STAP applications has been extensively discussed in [23].

Previous work [1]–[4], [8]–[11], [24] employed the GIP-based NHD for Gaussian interference scenarios. The GIP-based method relies on the statistics of a quadratic form given by $Q = \mathbf{x}^H\hat{\mathbf{R}}^{-1}\mathbf{x}$. This method can be used as an NHD test statistic in SIRV intereference if a perfect estimate of the covariance matrix can be obtained, which calls for an extremely large sample support size (infinite sample support). However, in practice, the training data available in a given application is limited by system considerations such as the bandwidth and fast scanning arrays and more fundamentally the underlying spatio-temporal nonstationarity of the scenario. Thus, one is almost always forced to work with finite sample support. Consequently, the covariance matrix estimate for this problem can only be obtained to within a constant of the sample covariance matrix, which is the maximum likelihood estimate of the covariance matrix underlying the Gaussian component of the SIRV. Typically, this constant is unknown in practice. Hence, the goodness-of-fit tests proposed in [3], [4], [9], and [10] cannot be properly implemented for this problem. On the other hand, implementation of the NHD tests proposed in [3], [4], [9]–[11], and [24] using the sample covariance matrix estimate for $\hat{\mathbf{R}}$ in SIRV scenarios leads to incorrect declaration of data nonhomogeneity. This fact is illustrated in the examples presented in Section IV. Therefore, we seek a scale-invariant test statistic for this problem.

III. Nonhomogeneity Detector for Non-Gaussian Interference Scenarios

Let $\mathbf{x} \sim \text{SIRV}[0,\mathbf{R},f_V(v)]$ denote the complex SIRV test data vector, where $\mathbf{R}$ is unknown. Further, let $\mathbf{x}_i$, $i = 1,2,\ldots K$, denote iid complex SIRV$[0,\mathbf{R},f_V(v)]$ training data. The first step in deriving the NHD for SIRV's involves obtaining the maximum likelihood estimate of the underlying covariance matrix. This estimate is then used in a test statistic that exhibits maximal invariance with respect to the unknown scaling of the estimated covariance matrix. The resulting test statistic takes the form of a normalized adaptive matched filter (NAMF), which has been extensively analyzed in [25]–[27] and references therein. As noted previously, the basis of our strategy to detect nonhomogeneity in the data is to first characterize the NHD PDF in homogeneous SIRP clutter scenarios and use this information to construct a formal goodness-of-fit test for rejecting data realizations that depart from the said PDF.

A. Covariance Matrix Estimation

The unknown covariance matrix is estimated from representative SIRV training data sharing the covariance structure of that of the test cell. Maximum likelihood (ML) estimation of the covariance matrix for SIRVs was first considered in [28]. The work of [28] showed that covariance matrix estimation for SIRVs can be treated in the framework of a complete-incomplete data problem and pointed out that the maximum likelihood estimate of the covariance matrix is a weighted sample matrix. Since the covariance matrix estimate cannot be obtained in closed form, [28], [29] use an iterative method known as the expectation-maximization (EM) algorithm. More precisely, let $\mathbf{x}_i, i = 1,2,\ldots,K$ denote iid training data sharing the covariance matrix of the test data vector $\mathbf{x}$. The work of [28] and [29] shows that the ML estimate of the covariance matrix is given by

$$\hat{\mathbf{R}} = \frac{1}{K}\sum_{i=1}^{K} c_i\mathbf{x}_i\mathbf{x}_i^H \tag{3}$$

where

$$c_i = -\frac{h'_{2M}(q_i)}{h_{2M}(q_i)}$$
$$h'_{2M}(w) = \frac{\partial h_{2M}(w)}{\partial w} = -h_{2M+2}(w) \tag{4}$$

and $q_i = \mathbf{x}_i^H \hat{\mathbf{R}}^{-1} \mathbf{x}_i$, $i = 1, 2, \ldots K$. Since both sides of (3) involve $\hat{\mathbf{R}}$ (the right-hand side implicitly through c_i), it is not possible to obtain the estimate in closed form. Consequently, [28] used the EM algorithm to obtain an iterative solution to the problem. We adopt the approach of [28] for obtaining the covariance matrix estimate in this work. A derivation of the covariance matrix estimate is contained in the Appendix. We note therein that the EM algorithm yields an estimate that is to within a multiplicative constant of the sample covariance matrix, which is the ML estimate of the covariance matrix underlying the Gaussian component of the SIRV. This fact was verified for all the simulated data examples presented in Section IV by examining the eigenvalues of the estimated covariance matrix obtained at the convergence of the EM algorithm. Details pertaining to the initial start and convergence properties of the EM algorithm can be found in [28]. The next step is to use this estimate in a maximally invariant decision statistic for nonhomogeneity detection.

Recognizing the need to know the characteristic SIRV PDF, which may be hard to obtain in some practical applications, the works of [30] and [31] propose recursive covariance matrix estimators for the class of non-Gaussian processes where the random variable V of the SIRP model is treated as a deterministic but unknown parameter. Strictly speaking, the non-Gaussian model used in [30] and [31] departs from the SIRP model due to the treatment of V as a deterministic but unknown scale factor. However, it serves as a useful alternative model in some instances.

B. Maximally Invariant NHD Test Statistic

The maximal invariant statistic for different scaling of test and training data is given by [25]

$$\Lambda_{\text{NAMF}} = \frac{|\mathbf{s}^H \hat{\mathbf{R}}^{-1} \mathbf{x}|^2}{[\mathbf{s}^H \hat{\mathbf{R}}^{-1} \mathbf{s}][\mathbf{x}^H \hat{\mathbf{R}}^{-1} \mathbf{x}]} \tag{5}$$

where $\mathbf{s} = (1/\sqrt{M})[1 \quad 1 \quad \ldots 1]^T$. For convenience, we use a simple choice for $\mathbf{s}$ by designating it to be the first column of a normalized discrete Fourier transform (DFT) matrix. However, in most STAP applications, the spatio-temporal steering vector is a function of azimuthal angle and Doppler. Bearing in mind that we are concerned about training data containing contaminating targets, which share the same angle-Doppler information as that of a desired target, the spatio-temporal steering vector is a logical choice for $\mathbf{s}$.

The test statistic of (5) has also been proposed as a suboptimal method for adaptive radar target detection in compound-Gaussian clutter [32]. Invariance properties of the test statistic of (5) and its geometrical representation have been studied in [25] and references therein for the case of Gaussian interference statistics using a sample covariance matrix estimate. In SIRP interference, however, each training data vector is scaled by a different realization of V. Since V varies independently from one training data vector to another, maximal invariance of the test statistic of (5) afforded by the sample covariance matrix estimate no longer applies. This is due to the fact that the sample covariance matrix is no longer the maximum likelihood estimate of the covariance matrix for SIRV scenarios [33].

However, using an estimated covariance matrix of the form of (3) restores the maximal invariance property of the test statistic of (5). This is due to the fact that the resultant covariance matrix estimate at convergence of the EM algorithm is to within a multiplicative constant of the sample covariance matrix. This fact is formally demonstrated in Section IV through simulation by comparing the empirical data cumulative distribution function (CDF) of a simple transformation on Λ_{NAMF} with its theoretical CDF for several cases and supplementing the results with a Kolmogorov–Smirnov test [34]. This behavior has also been verified for all the simulated data examples presented in Section IV by examining the eigenvalues of the estimated covariance matrix and the eigenvalues of the sample covariance matrix formed from the averaged outer products of the Gaussian component underlying the SIRV data. Consequently, we now have a case where the covariance matrix of the test and training data share the same structure but have different unknown scaling. It has been established in [25] that Λ_{NAMF} is the invariant test statistic for this problem. Hence, the canonical representation for Λ_{NAMF} in terms of five random variables derived in [25] applies to this problem in a straightforward manner. However, we emphasize that it is important to properly estimate the SIRV covariance matrix in order to reduce the NHD problem to the case where test and training data covariance matrices differ by an unknown scale factor. This calls for knowledge of the first order SIRV characteristic PDF.

C. PDF and Moments of the Non-Gaussian NHD Test Statistic

Our comments in the concluding paragraph of Section III-B allow us to use the canonical representation for Λ_{NAMF} contained in [25] for Gaussian interference scenarios. Consequently, the PDF of the NHD test statistic is readily determined in terms of a random variable Λ_{eq} obtained from a transformation on Λ_{NAMF} defined by

$$\Lambda_{\text{eq}} = \frac{\Lambda_{\text{NAMF}}}{1 - \Lambda_{\text{NAMF}}}. \tag{6}$$

Since Λ_{eq} is a monotonic function of Λ_{NAMF}, one can work with either statistic. For convenience of analysis, we work with the PDF of Λ_{eq} in the sequel. It has been shown in [25], [27], and [35] for Gaussian interference statistics that Λ_{eq} admits a representation in terms of an F-distributed random variable P and a beta-distributed loss factor Γ. However, use of the covariance matrix estimate of the form of (3) transforms the NHD problem in SIRV interference to that of testing whether two data sets share the same covariance structure with differing scale. Consequently, the results of [25], [27], and [35] readily extend to the SIRV problem. More precisely, for the case where no target is present in $\mathbf{x}$ (homogeneous data), Λ_{eq} admits a representation of the form

$$\Lambda_{\text{eq}} = \frac{P}{1 - \Gamma}. \tag{7}$$

The PDFs of P and Γ are given by

$$f_P(p) = \frac{L}{(1+p)^{L+1}} \quad p > 0$$
$$f_\Gamma(\gamma) = \frac{1}{\beta(L+1, M-1)} \gamma^L (1-\gamma)^{M-2} \quad 0 \le \gamma \le 1 \quad (8)$$

where $L = K - M + 1$, and

$$\beta(m,n) = \int_0^1 x^{m-1}(1-x)^{n-1} dx. \quad (9)$$

After a little bit of algebra, it follows that that the PDF of Λ_{eq} with no target present in $\mathbf{x}$ (homogeneous data) is given by

$$f_{\Lambda_{\text{eq}}}(r) = \int_0^1 \frac{L(1-\gamma) f_\Gamma(\gamma) d\gamma}{[1+(1-\gamma)r]^{L+1}} \quad (10)$$

while the pdf of Λ_{NAMF} with no target present in $\mathbf{x}$ (homogeneous data) is given by

$$f_{\Lambda_{\text{NAMF}}}(r) = \int_0^1 \frac{L(1-\gamma) f_\Gamma(\gamma) d\gamma}{[1+(1-\gamma)\frac{r}{1-r}]^{L+1}} \frac{1}{(1-r)^2}. \quad (11)$$

The mean of Λ_{NAMF} is difficult to calculate analytically. Consequently, we work with the mean of Λ_{eq} given by

$$E(\Lambda_{\text{eq}}) = \frac{K}{(K-M)(M-2)} \quad M > 2 \quad (12)$$

to study the convergence properties in the limit of large K. The statistical equivalence of Λ_{eq} to the ratio of an F-distributed random variable and a beta-distributed loss factor permits rapid calculation of the moments of Λ_{eq}. It is also extremely useful in Monte Carlo studies involving simulation of Λ_{NAMF}. For homogeneous training data, the use of (7) circumvents the need to explicitly generate the test data vector $\mathbf{x}$ and the training data vectors used for covariance estimation. For large M and, hence, large K, significant computational savings can be realized from the method of (7). It is instructive to note that the PDF of Λ_{eq} depends only on M and K, which are under the control of a system designer and not on nuisance parameters such as the true covariance matrix underlying the interference scenario. Furthermore, for $K \to \infty$, the mean of (12) converges to $E(\Lambda_{\text{eq}}) = 1/(M-2) \quad M > 2$, corresponding to the mean of an F-distributed random variable. This is due to the fact that as $K \to \infty$, the estimated covariance matrix approaches the true covariance matrix with probability one, and thus, the loss factor takes on the value zero with probability one.

D. Goodness-of-Fit Test

Since the PDF of Λ_{eq} and Λ_{NAMF} are known, a formal goodness-of-fit test can be used for nonhomogeneity detection in non-Gaussian interference scenarios. Specifically, the goodness-of-fit test can be cast in the form of the following statistical hypothesis test:

H_0 : Λ_{NAMF} is statistically consistent with the pdf of (11)

H_1 : Λ_{NAMF} is not statistically consistent with the pdf of (11).

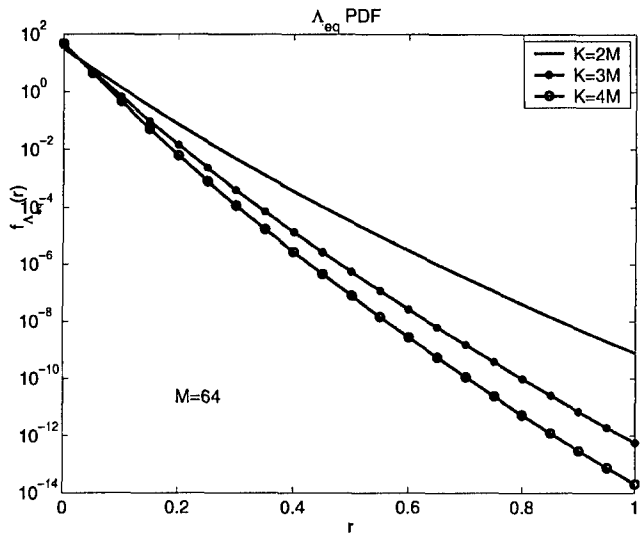

Fig. 1. Λ_{eq} PDF of (10) with varying K: M = 64.

For this purpose, we need to determine the type-I error [34] given by

$$P_e = P(\Lambda_{\text{NAMF}} > \eta | H_0) = P[\Lambda_{\text{eq}} > \frac{\eta}{(1-\eta)} | H_0]. \quad (13)$$

The type-I error is the probability of observing under H_0 a sample outcome at least as extreme as the one observed [34] and hence provides the smallest level at which the observed sample statistic is significant. Using (6) and (8), it follows that the probability of error conditioned on Γ is given by

$$P_e|\Gamma = \frac{1}{[1+(1-\gamma)\eta^*]^L} \quad (14)$$

where $\eta^* = \eta/(1-\eta)$. The unconditional type-I error probability is obtained by taking the expectation of (14) over Γ and is given by

$$P_e = \int_0^1 \frac{f_\Gamma(\gamma)}{[1+(1-\gamma)\eta^*]^L} d\gamma. \quad (15)$$

In this paper the type-I error is chosen to be 0.01. The threshold η^* is determined by a numerical inversion of (15). The value of η follows from the relationship $\eta = \eta^*/(1+\eta^*)$. We then form empirical realizations of Λ_{NAMF} from each training data vector using a sliding window approach. In this approach, each training data vector is treated as a test cell data vector, whose covariance matrix is estimated from neighboring cell data according to (3). We then test for statistical consistency of the realizations of Λ_{NAMF} with the theoretical PDF of (11). Realizations of Λ_{NAMF}, which exceed η, correspond to nonhomogeneous training data. A desirable feature of P_e is that it depends only on K and M and not on nuisance parameters such as the true covariance matrix underlying the interference. Performance analysis of the NHD method is presented in the next section.

IV. Performance Analysis

Performance of the goodness-of-fit test with simulated and measured data is presented here. Fig. 1 shows the plot of the

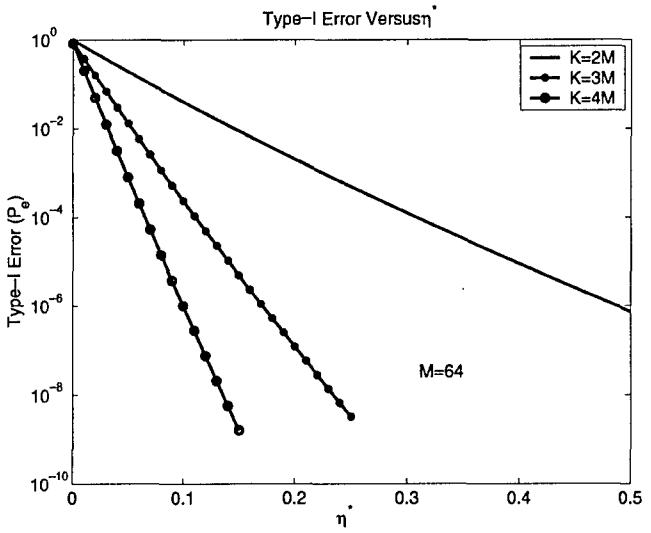

Fig. 2. Type-I Error versus η^* calculated using (15): M = 64.

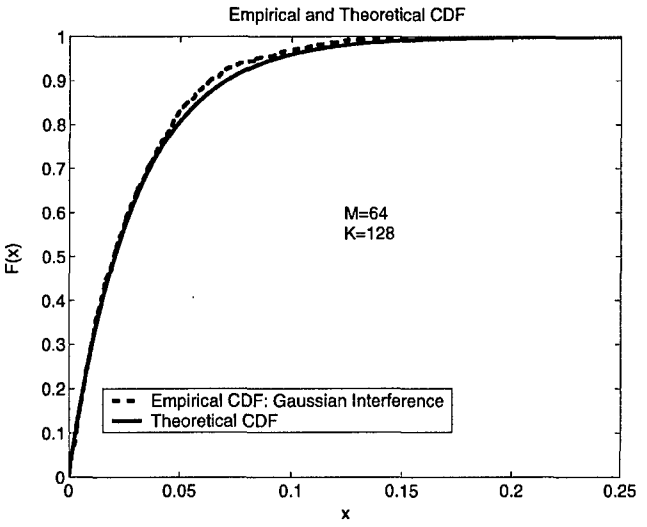

Fig. 3. Theoretical and empirical CDFs of Λ_{eq}: Gaussian interference.

PDF of Λ_{eq} obtained from (10) with K as a parameter. Observe that the variance of Λ_{eq} decreases with increasing K. This is due to the fact that better covariance matrix estimates result with increasing K and when $K \to \infty$, the estimated covariance matrix approaches $\mathbf{R}$ with probability 1.

Fig. 2 shows a plot of the Type-I error versus η^*, with K as a parameter. For a given type-I error, the threshold decreases with increasing K, in conformance with the results of Fig. 1.

For convenience of analysis, simulated data examples contained herein use the K-distributed amplitude PDF given by [12], [13], [21]

$$f_R(r) = \frac{b^{\alpha+1} r^{\alpha}}{2^{\alpha-1}\Gamma(\alpha)} K_{\alpha-1}(br) \quad r \geq 0,\ b,\ \alpha > 0 \qquad (16)$$

where b and α are the distribution scale and shape parameters, respectively, $K_\nu(.)$ is the modified Bessel function of the second kind of order ν, and $\Gamma(.)$ is the Eulero-Gamma function. The K-distribution, which is a member of the class of SIRPs [12], has been proposed as a model for impulsive clutter resulting from terrain and sea scatter [36], [37]. Small values of α result in heavy tails for the PDF of (16). The corresponding $f_V(v)$ and $h_{2M}(.)$ are given by

$$f_V(v) = \frac{2b}{\Gamma(\alpha)}(bv)^{2\alpha-1}\exp(-b^2v^2) \quad 0 \leq v \leq \infty$$
$$h_{2M}(w) = \frac{2b^{2M}}{\Gamma(\alpha)}(b\sqrt{w})^{\alpha-M}K_{\alpha-M}(2b\sqrt{w}). \qquad (17)$$

First, Figs. 3–5 demonstrate the invariance of the PDF of (10) for the K-distribution ($\alpha = 0.1, 0.5$) and the Gaussian case ($\alpha \to \infty$). More precisely, these figures show plots of the theoretical CDF obtained from (10) and the empirical CDF of Λ_{eq} formed from homogeneous simulated data using (6). Relevant test parameters are reported in the plots. First, the covariance matrix is estimated from $K = 2M$ homogeneous training data realizations using the EM algorithm discussed in Section III-A.

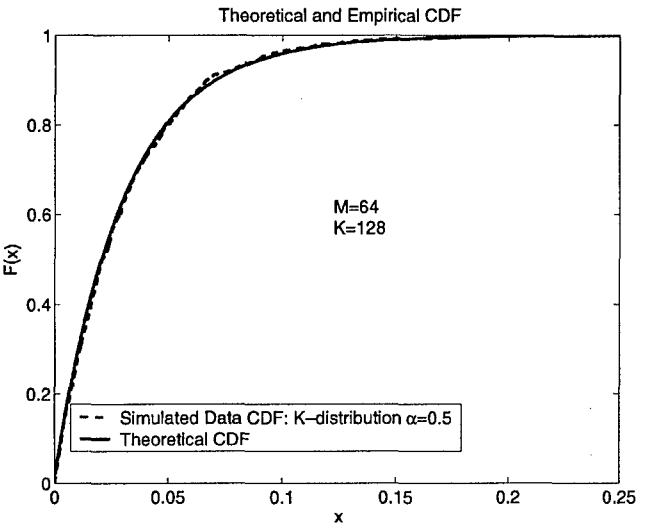

Fig. 4. Theoretical and empirical CDF's of Λ_{eq}: K-Distributed interference $\alpha = 0.5$.

Then, Λ_{eq} is formed using 1000 independent realizations of homogeneous data and its empirical CDF is compared to its theoretical CDF given by

$$F_{\Lambda_{eq}}(r) = 1 - \int_0^1 \frac{f_\Gamma(\gamma)}{[1+(1-\gamma)r]^L} d\gamma. \qquad (18)$$

In all cases, the empirical CDF shows good agreement with the theoretical CDF. This was further supplemented by performing a Kolmogorov–Smirnov test [34] to determine the statistical consistency of realizations of Λ_{eq} from the simulated data with the theoretical PDF of (10). In all cases, we could not reject the hypothesis that the realizations of Λ_{eq} formed from the simulated data using conform to the PDF of (10) at a 1% significance level. These findings confirm the scale invariance of Λ_{eq} (and, hence, Λ_{NAMF}) and verify the correctness of the PDF given by (10).

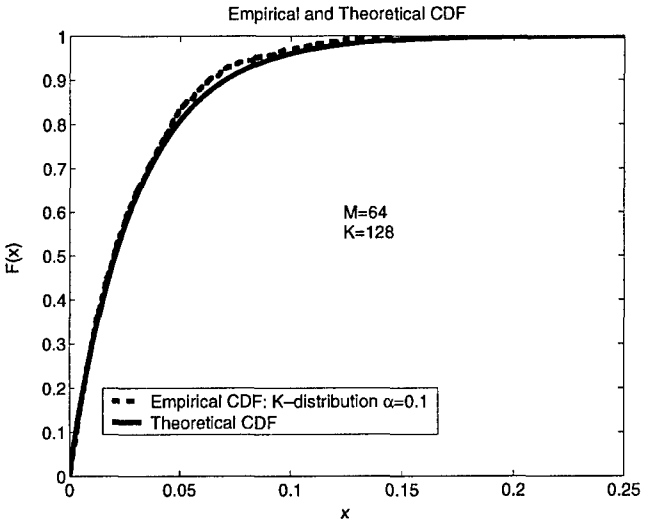

Fig. 5. Theoretical and empirical CDF's of Λ_{eq}: K-Distributed interference $\alpha = 0.1$.

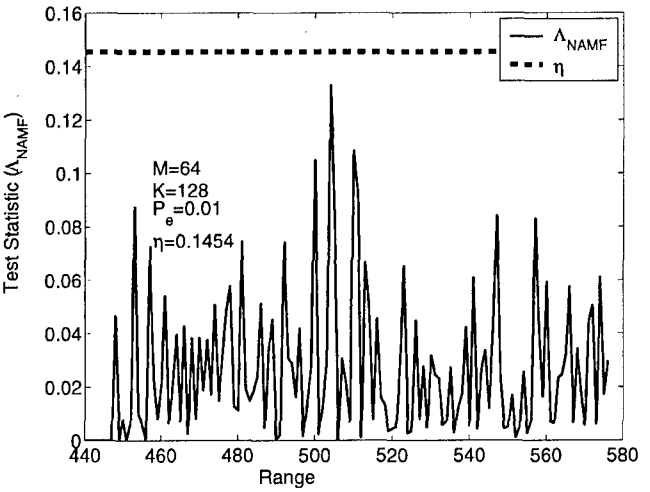

Fig. 6. Λ_{NAMF} versus range bin number for homogeneous K-distributed SIRV with $\alpha = 0.5$, $b = \sqrt{\alpha}$, M = 64, and K = 128.

We then generate 1024 realizations of a 64 tuple vector from the K-distributed SIRP with $\alpha = 0.5$ having a prescribed covariance matrix according to the physical model described in [38] using the approach of [13]. No targets are added to this data set. Starting from the midpoint (range bin 512), the data set is processed symmetrically on either side using a sliding window. Each cell is treated as a test cell (which may or may not contain contaminating targets). Two Guard cells are provided (one on each side of the test cell). One hundred and twenty eight training data realizations are collected by moving symmetrically on either side of the guard cells for use in covariance matrix estimation. The covariance matrix estimate is obtained using (3). Λ_{NAMF} given by (5) is then calculated for each test cell using the estimated covariance matrix and compared to a threshold determined from (15) for $P_e = 0.01$. Relevant test parameters are reported in the plots.

Fig. 6 shows the performance of the goodness-of-fit test for simulated homogeneous data from the K-distribution [21] with shape parameter 0.5 using the covariance estimate of (3). The

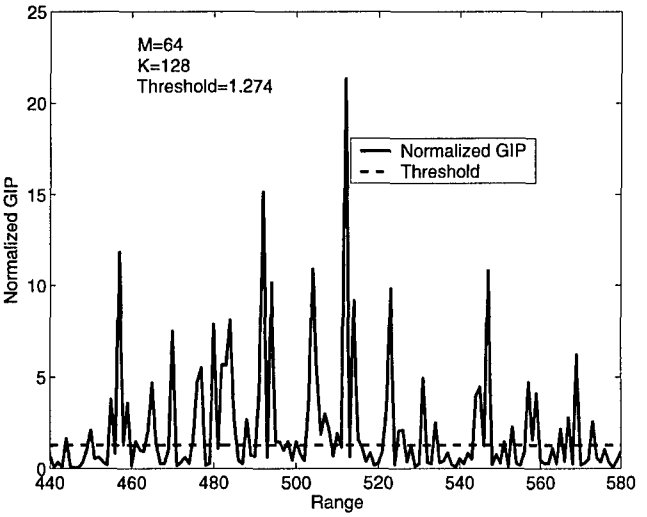

Fig. 7. Normalized GIP ($\mathbf{x}^H\mathbf{S}^{-1}\mathbf{x}/K$) versus range bin number for homogeneous K-distributed SIRV with $\alpha = 0.5$, $b = \sqrt{\alpha}$, M = 64, and K = 128.

figure shows a plot of Λ_{NAMF} as a function of range. No realization of Λ_{NAMF} exceeds η, reflecting homogeneity of the data. The experiment was repeated 1000 times, and in all cases, Λ_{NAMF} did not exceed η, confirming the homogeneity of the data.

Fig. 7 shows the performance of the NHD test proposed in [10], [11], and [24] based on comparing the normalized GIP $\mathbf{x}^H\mathbf{S}^{-1}\mathbf{x}/K$, with the threshold-setting determined according to [24, eq. (4.2)]. Here, $\mathbf{S} = (1/K)\sum_{i=1}^{K}\mathbf{x}_i\mathbf{x}_i^H$ is simply the sample covariance matrix. The data set used here is the same as the data set used for the example in Fig. 6. The normalized GIP is formed using sliding window processing, as described in [10], [11], and [24]. Fig. 7 shows a plot of the normalized GIP as a function of range. The threshold setting is also plotted. From the plot, it is evident that for almost all range bins the normalized GIP exceeds the threshold, leading to the declaration of nonhomogeneity, when in fact, the data is homogeneous.

Fig. 8 shows the performance of a second goodness-of-fit test proposed in [10], [11], and [24], which compares the normalized GIP $\mathbf{x}^H\mathbf{S}^{-1}\mathbf{x}/K$ to a theoretically calculated mean value obtained from [24, eq. (3.6)]. The data used for this example is the same as that used in the example of Fig. 6. Fig. 8 shows a plot of the normalized GIP as a function of range. The theoretically calculated mean value is also shown. Again, we see that for almost all range bins, the normalized GIP exceeds the mean value, causing an incorrect declaration of data nonhomogeneity.

Fig. 9 shows the performance of the NHD test proposed in [3], [4], and [9], which compares the GIP $\mathbf{x}^H\mathbf{S}^{-1}\mathbf{x}$ to a theoretically specified mean value of M. The data used for this example is the same as that used in the example of Fig. 6. Fig. 9 shows a plot of the GIP as a function of range. The theoretically specified mean value is also shown. Again, we see that for almost all range bins, the GIP exceeds the mean value causing an incorrect declaration of data nonhomogeneity. The incorrect declaration of nonhomogeneity is due to the fact that $\mathbf{S}$ is no longer the ML estimate of the covariance matrix for SIRV interference scenarios. Similar results showing an even more severe

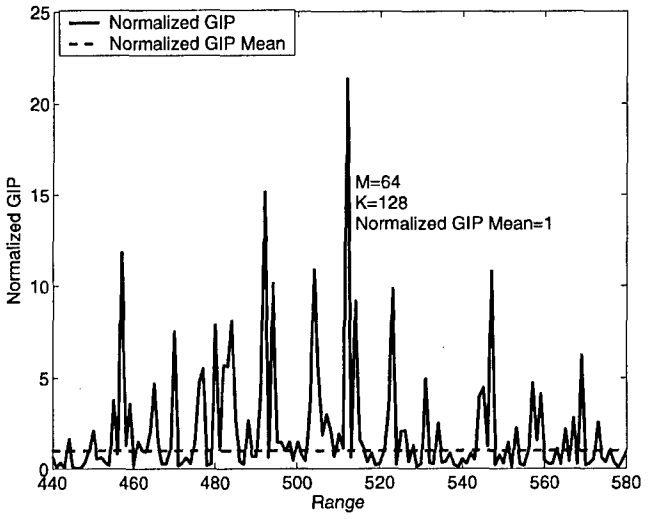

Fig. 8. Normalized GIP ($\mathbf{x}^H\mathbf{S}^{-1}\mathbf{x}/K$) versus range bin number for homogeneous K-distributed SIRV with $\alpha = 0.5, b = \sqrt{\alpha}$, M $= 64$, and K $= 128$.

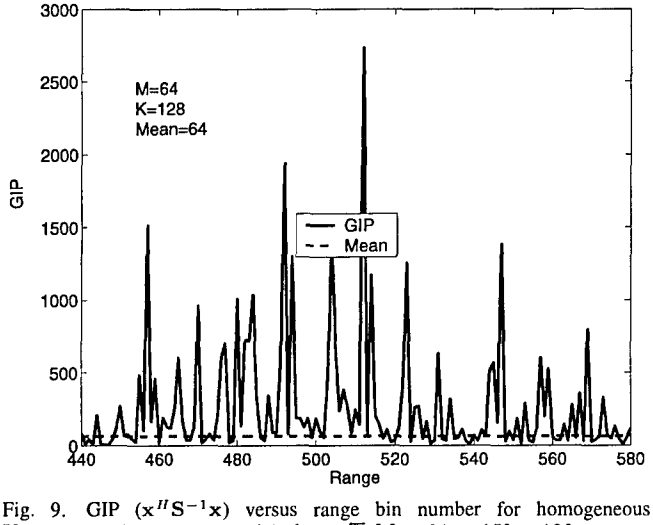

Fig. 9. GIP ($\mathbf{x}^H\mathbf{S}^{-1}\mathbf{x}$) versus range bin number for homogeneous K-distributed SIRV with $\alpha = 0.5, b = \sqrt{\alpha}$, M $= 64$, and K $= 128$.

performance degradation in K-distributed clutter with $\alpha = 0.1$ were obtained. However, these results are not reported here in the interest of avoiding tediousness of exposition. The experiments pertaining to Figs. 7–9 were repeated 1000 times, and all the trials exhibited performance consistent with that are reported in Figs. 7–9.

Fig. 10 shows the performance of the goodness-of-fit test developed in this paper in K-distributed clutter with shape parameter 0.5. Synthetic targets were injected at range bins 479 and 510 to cause the nonhomogeneity. Nonhomogeneity of the data is evident in those range bins where Λ_{NAMF} exceeds η.

Fig. 11 shows the performance of the goodness-of-fit test in K-distributed clutter with $\alpha = 0.1$. Synthetic targets were injected at range bins 510 and 552 to cause the nonhomogeneity. Clearly, Λ_{NAMF} exceeds η for both of these range bins, and thus, they are declared to be nonhomogeneous data sets.

Fig. 12 shows the results of the goodness-of-fit test using the covariance matrix estimator proposed in [30] and [31]. This estimator does not require knowledge of the first-order characteristic PDF of the SIRV and, therefore, converges faster than

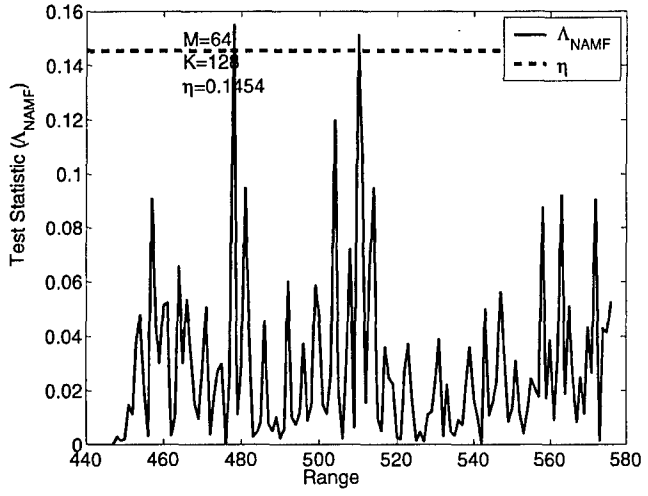

Fig. 10. Λ_{NAMF} versus range bin number for nonhomogeneous K-distributed SIRV with $\alpha = 0.5, b = \sqrt{\alpha}$, M $= 64$, and K $= 128$.

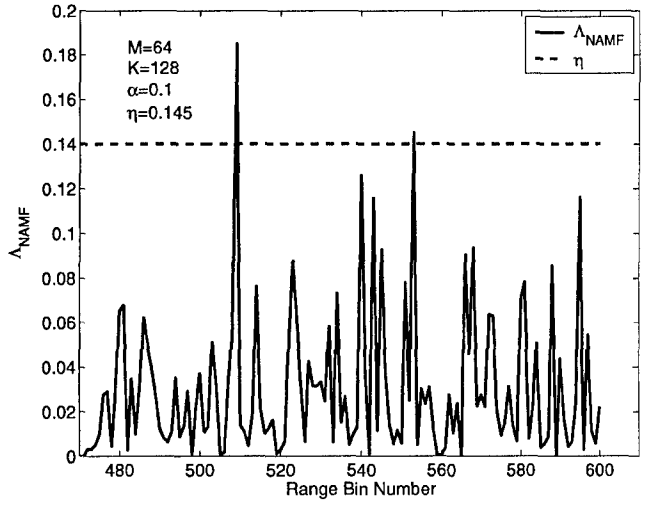

Fig. 11. Λ_{NAMF} versus range bin number for nonhomogeneous K-distributed SIRV with $\alpha = 0.1, b = \sqrt{\alpha}$, M $= 64$, and K $= 128$.

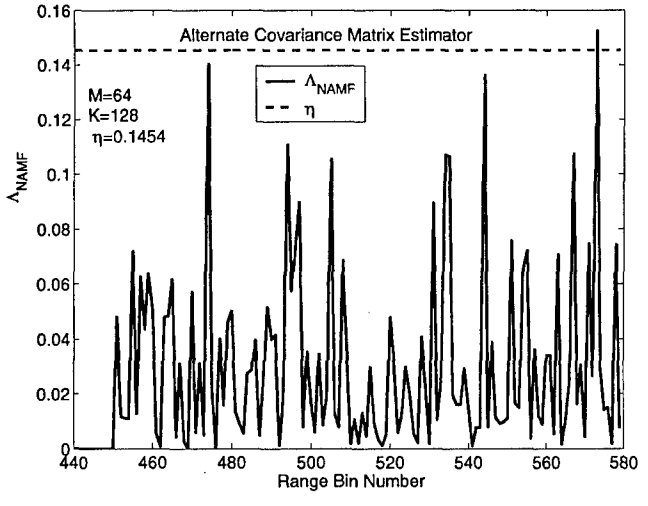

Fig. 12. Λ_{NAMF} versus range bin number for nonhomogeneous K-distributed SIRV with $\alpha = 0.5, b = \sqrt{\alpha}$, M $= 64$, K $= 128$, and the covariance matrix estimate of [30], [31].

TABLE I
NHD PERFORMANCE SUMMARY

Fig. Number	Range Bin	Realizations	Exceedences
10	510	1000	997
10	479	1000	997
11	510	1000	984
11	552	1000	984
12	573	1000	971

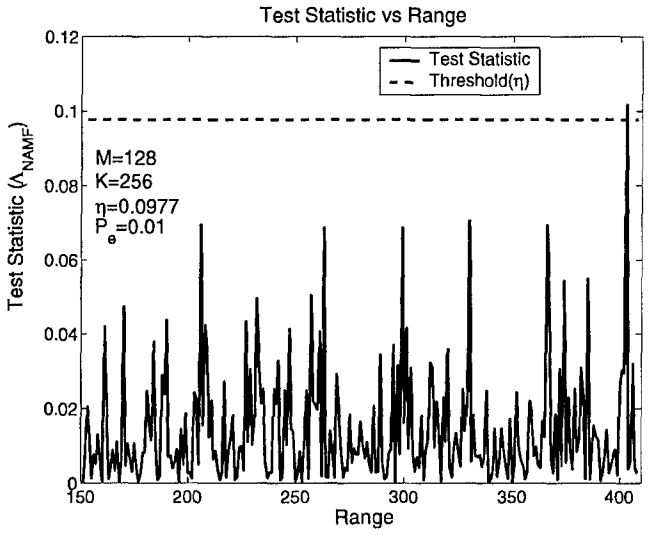

Fig. 13. Λ_{NAMF} versus range bin number using MCARM data: M = 128, K = 256.

the estimator of (3), especially for small values of α. The data set used for this example is the same as that used for the example in Fig. 10. Although a peak in the test statistic is seen at range bin 479, it does not exceed the threshold, whereas the peak is not seen for range bin 510. Therefore, contaminating targets in range bins 479 and 510 are not detected. Furthermore, the method erroneously reports the presence of a contaminating target at range bin 573. This illustrates the importance of knowing the underlying characteristic PDF to properly estimate the covariance matrix and use it in the NHD statistic.

The results contained in Figs. 10–12 were further validated by using 1000 realizations of the experiment and averaging the results over 50 independent trials. In 997 out of the 1000 trials, the NHD realizations corresponding to bins 479 and 510 of Fig. 10 exceeded the threshold. For Fig. 11, in 984 times out of 1000 trials, the realizations corresponding to range bins 510 and 552 exceeded the threshold. The corresponding number for Fig. 12 was 971. These findings are summarized in Table I.

The examples reported in Figs. 13–15 make use of the MCARM data [3]. The MCARM data consists of measured L-band radar data using a Westinghouse radar mounted on the port-side of a BAC1–11 aircraft. The relevant system parameters are summarized in Table II. The MCARM data is a common test bed for performance analysis and bench-marking of STAP algorithms and is therefore considered in this paper. Further details pertaining to the MCARM data can be found in [39]. Fig. 13 shows the results of the goodness-of-fit test for the MCARM data using acquisition 220 on Flight 5, cycle e for eight channels and 16 pulses. The results of [3], [40], and [41]

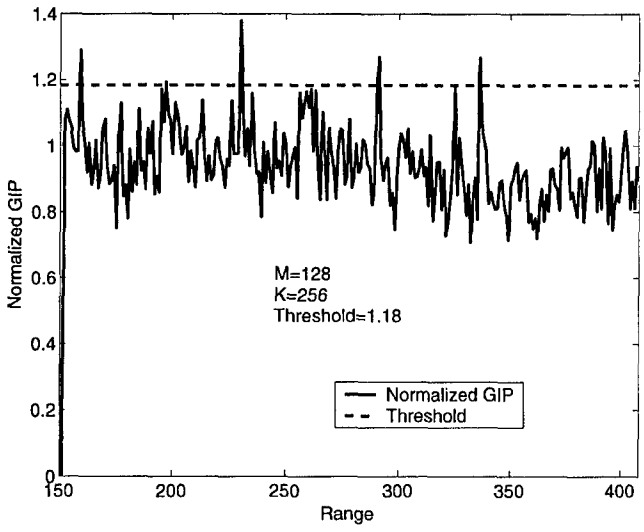

Fig. 14. Normalized GIP ($\mathbf{x}^H\mathbf{S}^{-1}\mathbf{x}/K$) versus range bin number using MCARM data: M = 128, K = 256.

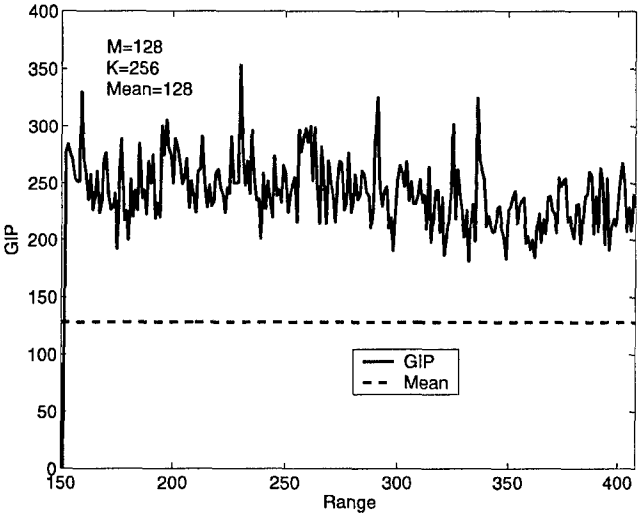

Fig. 15. GIP ($\mathbf{x}^H\mathbf{S}^{-1}\mathbf{x}$) versus range bin number using MCARM data: M = 128, K = 256.

TABLE II
MCARM DATA PARAMETERS

Parameter	Value
Transmit Frequency	1240 MHz
Transmit Beamwidth	6.7° Az., 10.4° El
Waveform	50.4 μs LFM
Peak Transmit Power	20 kw
Pulse Compression Ratio	63
Platform Altitude	10,000 ft
Platform Velocity	100 meters/sec
Array Configuration	11x11 Planar Array
Number of Pulses	128
Pulse Repetition Frequency	2 kHz
Number of Unambiguous Range Bins	630

using the MCARM tend to confirm that the MCARM data is homogeneous for the most part. Statistical analysis of the data indicates that the data is well-approximated by the Gaussian distribution [3]. As a consequence, $c_i = -h'_{2M}(q_i)/h_{2M}(q_i) = 1$ for this case. Hence, the maximum likelihood estimate of the

covariance matrix is simply the sample covariance matrix. The test statistic Λ_{NAMF} and the threshold η are plotted as a function of range. Nonhomogeneity of the data is evident in those bins for which Λ_{NAMF} exceeds η. For the sake of comparison, Figs. 14 and 15 show the performance of the NHD methods of [10], [11], and [24] and [3], [4], and [9], respectively, using the same MCARM data set used in the example of Fig. 13. Fig. 14 shows the results of the NHD test proposed in [10], [11], and [24] based on comparing the normalized GIP $\mathbf{x}^H\mathbf{S}^{-1}\mathbf{x}/K$ with the threshold setting determined according to [24, eq. (4.2)]. The MCARM data set is processed in the same manner as described in the example of Fig. 7. Fig. 15 shows the performance of the NHD test proposed in [3], [4], and [9], which compares the GIP $\mathbf{x}^H\mathbf{S}^{-1}\mathbf{x}$ to a theoretically specified mean value of M using the MCARM data. The MCARM data set is processed in the same manner as described in the example of Fig. 9. It is seen from Figs. 14 and 15 that a lot more declarations of nonhomogeneity result from the NHD methods of [10], [11], and [24] and [3], [4], and [9], when in fact the MCARM data is homogeneous. Thus, the NHD method of this paper outperforms competing techniques for Gaussian interference scenarios as well, in terms of the type-I error performance.

V. Conclusion

This paper provides a statistical characterization of the NHD for non-Gaussian interference scenarios, which can be modeled as a spherically invariant random process. A formal goodness-of-fit test based is derived. Performance analysis of the method is considered in some detail using simulated as well as measured data from the MCARM program. The performance comparison of the method with other NHD techniques is also undertaken. The illustrative examples validate the approach taken and confirm the improved performance of the technique of this paper in both Gaussian and non-Gaussian interference scenarios with respect to a type-I error criterion. Future work would include extensive performance analysis using simulated and measured data showing the resulting impact on STAP performance. The performance of several STAP algorithms in Gaussian and non-Gaussian interference scenarios has been considered in [26]. Future work will address performance of the methods treated in [26] in conjunction with NHD processing described herein to combat heterogeneous interference scenarios. Preliminary work (not reported here) in this direction reveals that the estimator of (3) is rather slow to converge, even for moderate system dimension. A related research direction is the performance comparison of model-based parametric STAP methods (which do not require NHD preprocessing) with sample covariance-based STAP methods employing NHD preprocessing in dense target environments. Analysis in this direction is undertaken in [42].

Appendix
EM Algorithm for Covariance Matrix Estimation

We discuss the maximum likelihood estimation of the SIRV covariance matrix in this appendix. Let $\mathbf{X}$ denote a data matrix, whose columns $\mathbf{x}_i$ $i = 1, 2, \ldots, K$ are iid training data vectors, which are distributed as SIRV$[0, \mathbf{R}_x, f_V(v)]$. The likelihood function for estimating $\mathbf{R}$ is given by

$$g[\mathbf{X}|\mathbf{R}] = \prod_{i=1}^{K} \pi^{-M}|\mathbf{R}|^{-1}h_{2M}(q_i). \tag{19}$$

Direct maximization of the likelihood function of (19) over $\mathbf{R}$ is rendered difficult due to the fact that there is missing information. Consequently, it is helpful to treat the problem in the context of a complete-incomplete data problem [28]. Recall from the representation theorem for SIRVs [22] that $\mathbf{x}_i = \mathbf{z}_i V_i$, where $\mathbf{z}_i$, $i = 1, 2, \ldots, K$ are statistically independent $CN(0, \mathbf{R})$ random vectors, and V_i $i = 1, 2, \ldots, K$ are statistically independent random variables with PDF $f_V(v)$. For this problem, the complete data is either $\mathbf{z}_i$, V_i, $i = 1, 2, \ldots, K$, or $\mathbf{x}_i$, V_i, $i = 1, 2, \ldots, K$. However, the observed data $\mathbf{x}_i$, $i = 1, 2, \ldots, K$ contains no explicit information about V_i, $i = 1, 2, \ldots, K$ and, thus, constitutes the incomplete data. The complete data likelihood function is given by the joint PDF of $\mathbf{x}_i$, V_i, $i = 1, 2, \ldots, K$, which is expressed as

$$g_c[\mathbf{X}, V_i|\mathbf{R}] = \prod_{i=1}^{K} f(\mathbf{x}_i|V_i) \prod_{i=1}^{K} f(v_i). \tag{20}$$

Taking the natural logarithm of (20) yields the complete-data log-likelihood function of the form

$$L[\mathbf{X}, V_i|\mathbf{R}] = -KM\log(\pi) - K\log(|\mathbf{R}|) - \sum_{i=1}^{K} q_i v_i^{-2} + \sum_{i=1}^{K} \log[v_i^{-2M} f(v_i)]. \tag{21}$$

Note that given an initial estimate of $\mathbf{R}$ denoted by $\hat{\mathbf{R}}$, the quantity

$$E\{\log[v_i^{-2M} f(v_i)]|\hat{\mathbf{R}}\} \tag{22}$$

depends only on $\hat{\mathbf{R}}$ and not on $\mathbf{R}$. Consequently, the relevant terms for the maximization over $\mathbf{R}$ are given by

$$L_1[\mathbf{X}, V_i|\mathbf{R}] = -K\log(|\mathbf{R}|) - \sum_{i=1}^{K} q_i v_i^{-2}. \tag{23}$$

The missing data v_i, $i = 1, 2, \ldots K$ are assumed to be missing at random (MAR) [28]. Consequently, given an initial estimate of $\mathbf{R}$ denoted by $\hat{\mathbf{R}}$, the complete data sufficient statistic [28] is given by

$$c_i = E[V_i^{-2}|\hat{\mathbf{R}},\ \mathbf{x}_i]. \tag{24}$$

Thus, c_i is simply the minimum mean squared error (MMSE) estimate of V_i^{-2} given $\mathbf{x}_i$. Note that $f(v_1) = f(v_2) = \cdots = f(v_K) = f_V(v)$ (since v_i, $i = 1, 2, \ldots K$ are iid random variables). Therefore

$$f_{V_i|\mathbf{x}_i,\ \hat{\mathbf{R}}}(v_i|\mathbf{x}_i,\ \hat{\mathbf{R}}) = \frac{f(\mathbf{x}_i|v_i,\ \hat{\mathbf{R}})f_V(v_i)}{f_{\mathbf{x}_i|\hat{\mathbf{R}}}(\mathbf{x}_i|\hat{\mathbf{R}})}. \tag{25}$$

However

$$\frac{f(\mathbf{x}_i|v_i,\ \hat{\mathbf{R}})f_V(v_i)}{f_{\mathbf{X}_i|\hat{\mathbf{R}}}(\mathbf{x}_i|\hat{\mathbf{R}})} = \frac{v_i^{-2M}\exp(q_i v_i^{-2})f_V(v_i)}{h_{2M}(q_i)}. \quad (26)$$

Consequently

$$\begin{aligned} c_i &= \frac{\int_0^\infty v_i^{-2M-2}\exp(q_i v_i^{-2})f_V(v_i)dv_i}{h_{2M}(q_i)} \\ &= -\frac{h'_{2M}(q_i)}{h_{2M}(q_i)} \\ &= \frac{h_{2M+2}(q_i)}{h_{2M}(q_i)}. \end{aligned} \quad (27)$$

Having specified the complete data sufficient statistic, we seek the maximization of (23). For this purpose, we reproduce the following matrix differentiation identities from [43]:

$$\begin{aligned} \delta[\mathbf{R}^{-1}] &= -\mathbf{R}^{-1}\delta[\mathbf{R}]\mathbf{R}^{-1} \\ \delta[\log|\mathbf{R}^{-1}|] &= -\mathrm{tr}\{\mathbf{R}^{-1}\delta[\mathbf{R}]\}. \end{aligned} \quad (28)$$

Further, we recognize that $q_i = \sum_{i=1}^K \mathrm{tr}[\mathbf{R}^{-1}\mathbf{x}_i\mathbf{x}_i^H]$. Consequently

$$\delta L_1[\mathbf{X}, V_i|\mathbf{R}] = K\mathrm{tr}\{\mathbf{R}^{-1}\delta[\mathbf{R}]\} - \mathrm{tr}[\mathbf{R}^{-1}\delta[\mathbf{R}]\mathbf{R}^{-1}\sum_{i=1}^K c_i\mathbf{x}_i\mathbf{x}_i^H]. \quad (29)$$

Maximization of (23) results from setting (29) equal to zero. Therefore, the maximum likelihood estimate of $\mathbf{R}$ is given by

$$\hat{\mathbf{R}} = \frac{1}{K}\sum_{i=1}^K c_i\mathbf{x}_i\mathbf{x}_i^H. \quad (30)$$

Since $\hat{\mathbf{R}}$ appears on both sides of (30) (implicitly on the right-hand side through the calculation of c_i), it is not possible to obtain a closed form solution for the resulting estimate. Consequently, an iterative method is needed for calculating $\hat{\mathbf{R}}$. The EM algorithm, which provides an iterative solution to this problem, is summarized below.

1) *E-Step:* Given an initial estimate of $\mathbf{R}$ denoted by $\hat{\mathbf{R}}$, calculate c_i for $i = 1, 2, \ldots, K$.
2) *M-Step:* Calculate $\hat{\mathbf{R}} = (1/K)\sum_{i=1}^K c_i\mathbf{x}_i\mathbf{x}_i^H$.
3) Use $\hat{\mathbf{R}}$ from Step 2 to calculate a new value of c_i.
4) Iterate until convergence. Convergence is determined through a suitable error criterion.

In this paper, the convergence criterion is an error of 10^{-6} defined to be the Frobenius norm of the difference between the values of $\hat{\mathbf{R}}$ resulting from two successive iterations. At convergence, the resultant $\hat{\mathbf{R}}$ is to within a multiplicative constant of the sample covariance matrix. This is due to the fact that the outer product of each training data realization with itself is scaled by the MMSE estimate of V_i^{-2}. This fact has been verified for all the simulated data examples presented in the paper. In particular, we examined the diagonal matrix of eigenvalues of the estimated covariance matrix. We found that they were to within a multiplicative constant of the eigenvalues of the sample covariance matrix formed by averaging the outer products of the realizations $\mathbf{z}_i$, $i = 1, 2, \ldots, K$ of the Gaussian component of the SIRV $\mathbf{x}_i$. Convergence of the algorithm is dictated by the choice of the initial estimate of $\mathbf{R}$. Any positive definite Hermitian matrix is suitable for the initial estimate of $\mathbf{R}$. Two choices that readily arise are the $M \times M$ identity matrix $\mathbf{I}_M$ and the sample covariance matrix given by $\mathbf{S} = (1/K)\sum_{i=1}^K \mathbf{x}_i\mathbf{x}_i^H$. We employ the latter choice in this paper due to the fact that it yields faster convergence.

The simulated data examples in this paper employing the covariance matrix estimate of (3) involve a calculation of the modified Bessel function of the second kind for specifying $h_{2M}(.)$ and its derivative. Numerical errors in their calculation for $\alpha = 0.1$ tend to be rather large. Consequently, convergence of the algorithm is extremely slow for $\alpha = 0.1$.

REFERENCES

[1] P. Chen, ""On testing the equality of covariance matrices under singularity," Tech. Rep.," AFOSR Summer Faculty Res. Program, Rome Lab., Rome, NY, 1994.
[2] ——, ""Partitioning Procedure in Radar Signal Processing Problems," tech. rep.," AFOSR Summer Faculty Research Program, Rome Laboratory, 1995.
[3] W. L. Melvin, M. C. Wicks, and R. D. Brown, "Assessment of multichannel airborne radar measurements for analysis and design of space-time adaptive processing architectures and algorithms," in *Proc. IEEE Nat. Radar Conf.*, Ann Arbor, MI, 1996.
[4] W. L. Melvin and M. C. Wicks, "Improving practical space-time adaptive radar," in *Proc. IEEE Nat. Radar Conf.*, Syracuse, NY, 1997.
[5] W. L. Melvin, "Space-time adaptive radar performance in heterogenous clutter," *IEEE Trans. Aerosp. Electron. Syst.*, vol. 36, no. 2, pp. 621–633, Apr. 2000.
[6] R. Nitzberg, "An effect of range-heterogenous clutter on adaptive Doppler filters," *IEEE Trans. Aerosp. Electron. Syst.*, vol. 26, no. 3, pp. 475–480, May 1990.
[7] W. L. Melvin, J. R. Guerci, M. J. Callahan, and M. C. Wicks, "Design of adaptive detection algorithms for surveillance radar," in *Proc. Int. Radar Conf.*, Alexandria, VA, 2000.
[8] B. Himed, Y. Salama, and J. H. Michels, "Improved detection of close proximity targets using two-step NHD," in *Proc. Int. Radar Conf.*, Alexandria, VA, 2000.
[9] P. Chen, W. L. Melvin, and M. C. Wicks, "Screening among multivariate normal data," *J. Multivariate Anal.*, vol. 69, pp. 10–29, 1999.
[10] M. Rangaswamy, B. Himed, and J. H. Michels, "Statistical analysis of the nonhomogeneity detector," in *Proc. 34th Asilomar Conf. Signals, Syst., Comput.*, Pacific Grove, CA, 2000.
[11] ——, "Performance analysis of the nonhomogeneity detector for STAP applications," in *Proc. IEEE Radar Conf.*, Atlanta, GA, May 2001.
[12] M. Rangaswamy, D. D. Weiner, and A. Ozturk, "Non-Gaussian random vector identification using spherically invariant random processes," *IEEE Trans. Aerosp. Electron. Syst.*, vol. 29, pp. 111–124, Jan. 1993.
[13] ——, "Computer generation of correlated non-Gaussian radar clutter," *IEEE Trans. Aerosp. Electron. Syst.*, vol. 31, no. 1, pp. 106–116, Jan. 1995.
[14] K. J. Sangston and K. R. Gerlach, "Coherent detection of radar targets in a non-Gaussian background," *IEEE Trans. Aerosp. Electron. Syst.*, vol. 30, no. 2, pp. 330–340, Apr. 1994.

[15] M. Rangaswamy, F. C. Lin, and K. R. Gerlach, "Robust adaptive signal processing methods for heterogeneous radar clutter scenarios," in *Proc. IEEE Radar Conf.*, Huntsville, AL, May 2003.
[16] Y.-L. Wang, J.-W. Chen, Z. Bao, and Y.-N. Peng, "Robust space-time adaptive processing for airborne radar in nonhomogeneous clutter environments," *IEEE Trans. Aerosp. Electron. Syst.*, vol. 39, no. 1, pp. 70–81, Jan. 2003.
[17] J. R. Guerci and J. S. Bergin, "Principal components, covariance matrix tapers, and the subspace leakage problem," *IEEE Trans. Aerosp. Electron. Syst.*, vol. 38, no. 1, pp. 152–162, Jan. 2002.
[18] K. R. Gerlach, "Outlier resistant adaptive matched filtering," *IEEE Trans. Aerosp. Electron. Syst.*, vol. 38, no. 3, pp. 885–901, Jul. 2002.
[19] S. A. Vorobyov, A. B. Gershman, and Z. Q. Luo, "Robust adaptive beamforming using worst-case performance optimization: A solution to the signal mismatch problem," *IEEE Trans. Signal Process.*, vol. 51, no. 2, pp. 313–324, Feb. 2003.
[20] K. J. Sangston and K. Gerlach, ""Non-Gaussian Noise Models and Coherent Detection of Radar Targets," Tech. Rep.," Naval Res. Lab., Washington, DC, 1992.
[21] M. Rangaswamy, J. H. Michels, and D. D. Weiner, "Multichannel detection for correlated non-Gaussian random processes based on innovations," *IEEE Trans. Signal Processing*, vol. 43, no. 8, pp. 1915–1922, Aug. 1995.
[22] K. Yao, "A representation theorem and its applications to spherically invariant random processes," *IEEE Trans. Inf. Theory*, vol. IT-19, no. 5, pp. 600–608, Sep. 1973.
[23] N. B. Pulsone, "Adaptive Signal Detection in Non-Gaussian Interference," Ph.D. dissertation, Northeastern Univ., Boston, MA, 1997.
[24] M. Rangaswamy, J. H. Michels, and B. Himed, "Statistical analysis of the nonhomogeneity detector for STAP applications," *Digit. Signal Process.*, vol. 14, no. 3, 2004.
[25] S. Kraut, L. L. Scharf, and L. T. McWhorter, "Adaptive subspace detectors," *IEEE Trans. Signal Process.*, vol. 49, no. 1, pp. 1–16, Jan. 2001.
[26] J. H. Michels, B. Himed, and M. Rangaswamy, "Performance of STAP tests in Gaussian and compound-Gaussian clutter," *Digit. Signal Process.*, vol. 10, no. 4, pp. 309–324, 2000.
[27] J. H. Michels, M. Rangaswamy, and B. Himed, "Performance of parametric and covariance based STAP tests in compound-Gaussian clutter," *Digit. Signal Process.*, vol. 12, no. 2,3, pp. 307–328, 2002.
[28] R. J. A. Little and D. B. Rubin, *Statistical Analysis with Missing Data*. New York: Wiley, 1987.
[29] M. Rangaswamy and J. H. Michels, "Adaptive processing in non-Gaussian noise backgrounds," in *Proc. Ninth IEEE Workshop Statist. Signal Array Process.*, Portland, OR, 1998.
[30] E. Conte, A. DeMaio, and G. Ricci, "Recursive estimation of the covariance matrix of a compound-Gaussian process and its application to adaptive CFAR," *IEEE Trans. Signal Processing*, vol. 50, no. 8, pp. 1908–1916, Aug. 2002.
[31] F. Gini and M. Greco, "Covariance matrix estimation for CFAR detection in correlated heavy tailed clutter," *Signal Process.*, vol. 82, no. 12, pp. 1847–1859, 2002.
[32] ——, "Suboptimum approach to adaptive coherent radar detection in compound-Gaussian clutter," *IEEE Trans. Aerosp. Electron. Syst.*, vol. 35, no. 3, pp. 1095–1103, Jul. 1999.
[33] F. Gini and J. H. Michels, "Performance analysis of two covariance matrix estimators in compound Gaussian clutter," *Proc. Inst. Elect. F. Radar, Sonar Navigat.*, vol. 146, no. 3, pp. 133–140, 1999.
[34] V. K. Rohatgi, *Statistical Inference*. Mineola, NY: Dover, 2003.
[35] J. H. Michels, M. Rangaswamy, and B. Himed, "Performance of STAP tests in compound Gaussian clutter," in *Proc. First IEEE Workshop Sensor Array Multichan. Process.*, Cambridge, MA, 2000.
[36] E. Jakeman and P. N. Pusey, "A model for non-Rayleigh sea echo," *IEEE Trans. Antennas Propag.*, vol. AP-24, no. 6, pp. 806–814, Nov. 1976.
[37] J. K. Jao, "Amplitude distribution of composite terrain radar clutter and the K-distribution," *IEEE Trans. Antennas Propag.*, vol. AP-32, no. 10, pp. 1049–1062, Oct. 1984.
[38] J. H. Michels, T. Tsao, B. Himed, and M. Rangaswamy, "Space-time adaptive processing (STAP) in airborne radar applications," in *Proc. IASTED Conf. Signal Process. Commun.*, Canary Islands, Spain, 1998.
[39] Data from the Multichannel Airborne Radar Measurement Program of the U.S. Air Force Research Laboratory. MCARMDATA, Rome, NY. [Online]. Available: www@http://128.132.2.229
[40] B. Himed and W. L. Melvin, "Analyzing space-time adaptive processors using measured data," in *Proc. 31st Asilomar Conf. Signals, Syst., Comput.*, Pacific Grove, CA, 1997.
[41] X. Lin and R. S. Blum, "Robust STAP algorithms using prior knowledge for airborne radar application," *Signal Process.*, vol. 79, pp. 273–287, 1999.
[42] J. H. Michels, M. Rangaswamy, and B. Himed, "Robust multichannel detection in heterogeneous airborne radar disturbance," in *Proc. IEEE Radar Conf.*, Long Beach, CA, Apr. 2002.
[43] J. P. Burg, D. G. Luenberger, and D. L. Wenger, "Estimation of structured covariance matrices," *Proc. IEEE*, vol. 70, pp. 963–974, 1982.

Muralidhar Rangaswamy (S'89–M'93–SM'98) received the B.E. degree in electronics engineering from Bangalore University, Bangalore, India, in 1985 and the M.S. and Ph.D. degrees in electrical engineering from Syracuse University, Syracuse, NY, in December 1992.

He was a Post-Doctoral Research Associate of the National Research Council between March 1993 and March 1994 at the Rome Laboratory, U.S. Air Force, Hanscom Air Force Base, MA. He is currently a Senior Electronics Engineer at the U.S. Air Force Research Laboratory, Hanscom Air Force Base. Prior to this, he held several academic and industrial appointments. His research interests include radar signal processing, spectrum estimation, modeling non-Gaussian interference phenomena, and statistical communication theory. He has authored numerous journal and conference papers in the areas of his research interests. He is a co-inventor on two U.S. patents in the areas of his research interests.

Dr. Rangaswamy presented invited papers at the Asilomar Conference on Signals, Systems, and Computers, Pacific Grove, CA, in November 1993; the AFOSR/DSTO Workshop, Victor Harbour, Australia, in June 1997; the Conference on Information Sciences and Systems, Princeton, NJ, in March 1998; the Asilomar Conference on Signals, Systems, and Computers, in November 2003; and the International Symposium on Signal Processing and Information Technology, Damstadt, Germany, in December 2003. He coauthored one chapter in the book *Introduction to Ultra-Wideband Radar Systems* (Boca Raton, FL: CRC, 1995) and one chapter in the book *Defence Applications of Signal Processing* (Amsterdam, The Netherlands: Elsevier Science B.V., 2001). He has delivered numerous invited seminars at academic, industrial, and governmental forums. He served as guest lecturer for the IEEE-AES Society Boston Chapter lectures in October 1999 and December 2000. He offered short courses on space-time adaptive processing for the IEEE AES Society in Boston (April 2003) and Atlanta (March 2004). He is a member of the editorial board of the *Digital Signal Processing* journal. He serves as an associate member of the sensor array and multichannel processing technical committee of the IEEE Signal Processing society and regularly performs peer review for several IEEE transactions.